Macalester Journal of Physics and Astronomy

Volume 1
Issue 1 *Spring 2013*

Article 10

May 2013

SHIELD: Star Formation from WIYN and GALEX Imaging

Samilee J. Moody
Macalester College, samilee.moody@gmail.com

SHIELD: Star Formation from WIYN and GALEX Imaging

Abstract

Using images from the *GALEX* (Galaxy Evolution Explorer) GR6 pipeline (released 2010), as well as the *WIYN* 3.5m Observatory, we present a survey of the twelve SHIELD galaxies in the far-ultraviolet (FUV, 1500 Å) and near-ultraviolet (NUV, 2200 Å) filters. FUV data were available for eleven of the galaxies, AGC 749237 being the exception. Aperture photometry was performed on each image to determine the AB magnitude in the FUV and NUV filters.These values were then used to calculate flux, luminosity, and star formation rates (SFRs). Similarly, Hα images of each galaxy from *WIYN* (omitting AGC 749241) were analyzed to determine an SFR from Hα tracers. A comparison of the two star formation indicators for these galaxies suggests the presence of an Hα detriment, and supports previous findings regarding refined conversions for SFRs in extremely low-mass dwarfs.

Keywords

galaxies: dwarf - galaxies: evolution - galaxies: irregular, galaxies: photometry

Cover Page Footnote

The author acknowledges these contibutors: John M. Cannon, Macalester College, Saint Paul, MN, 55105 Ian Cave, Macalester College, Saint Paul, MN, 55105 Elise Larson, Macalester College, Saint Paul, MN, 55105 Melissa Marshall, Macalester College, Saint Paul, MN, 55105 Elizabeth A.K. Adams, Cornell University, Ithaca, NY, 14850 Andrew E. Dolphin, Raytheon E.C. Elson, ICRAR/UWA Riccardo Giovanelli, Cornell University, Ithaca, NY, 14850 Martha P. Haynes, Cornell University, Ithaca, NY, 14850 Kristen B. McQuinn, University of Minnesota, Minneapolis, MN, 55455 Juergen Ott, NRAO Amelie Saintonge, Max Planck-Institute, Munich, Germany John J. Salzer, Indiana University, Bloomington, IN, 47405 Evan D. Skillman, University of Minnesota, Minneapolis, MN, 55455

SHIELD: Star Formation from *WIYN* and *GALEX* Imaging

Samilee J. Moody[1], John M. Cannon[1], Ian Cave[1], Elise Larson[1], Melissa Marshall[1], Elizabeth A.K. Adams[2], Andrew E. Dolphin[3], E.C. Elson[4], Riccardo Giovanelli[2], Martha P. Haynes[2], Kristen B. McQuinn[5], Juergen Ott[6], Amelie Saintonge[7], John J. Salzer[8], Evan D. Skillman[5]

ABSTRACT

Using images from the *GALEX* (Galaxy Evolution Explorer) GR6 pipeline (released 2010), as well as the *WIYN* 3.5m Observatory, we present a survey of the twelve SHIELD galaxies in the far-ultraviolet (FUV, 1500 Å) and near-ultraviolet (NUV, 2200 Å) filters. FUV data were available for eleven of the galaxies, AGC 749237 being the exception. Aperture photometry was performed on each image to determine the AB magnitude in the FUV and NUV filters. These values were then used to calculate flux, luminosity, and star formation rates (SFRs). Similarly, Hα images of each galaxy from *WIYN* (omitting AGC 749241) were analyzed to determine an SFR from Hα tracers. A comparison of the two star formation indicators for these galaxies suggests the presence of an

[1]Macalester College, Saint Paul, MN, 55105

[2]Cornell University, Ithaca, NY, 14850

[3]Raytheon

[4]ICRAR/UWA

[5]University of Minnesota, Minneapolis, MN, 55455

[6]NRAO

[7]Max Planck-Institute, Munich, Germany

[8]Indiana University, Bloomington, IN, 47405

Hα detriment, and supports previous findings regarding refined conversions for SFRs in extremely low-mass dwarfs.

Subject headings: galaxies: dwarf - galaxies: evolution - galaxies: irregular - galaxies: photometry - galaxies: photometry

1. Introduction

Measuring the star formation rate of a galaxy provides a glimpse into its evolution and history. The star formation rate (SFR) of a galaxy is determined through ultraviolet (UV) non-ionizing continuum flux and Hα nebular line emission. FUV and Hα SFRs are the two most fundamental and widely-discussed SFR metrics, and therefore are the focus of this analysis. UV flux is the result of photospheric emission from O- and late B-type stars, and tracks star formation on timescales $\backsim 10^8$ yr. Hα emission is a tracer of ionized hydrogen gas in the most massive, hot, and young stars, $M_* \gtrsim 17\ M_\odot$(Lee et al. 2009). These values are measured directly from the FUV or Hα luminosity of a galaxy. Since the hot stars from which Hα emission originates are short-lived, Hα SFRs become a primary indicator of short-term star formation. However, some surveys (Lee et al. 2009) have concluded that the Hα under-predicts the SFR relative to the FUV calculation. It is unclear why this trend exists, although dust attenuation, irregular star formation histories (SFHs), and non-solar metallicities have all been examined as potential causes.

The Survey of HI in Extremely Low-Mass Dwarfs (SHIELD) sample consists of twelve galaxies with HI masses between 10^6 and $10^7\ M_\odot$, a project conceived from the Arecibo Legacy Fast Arecibo L-band Feed Array (*ALFALFA*) Survey (Giovanelli et al. 2005). Studying low-mass galaxies is crucial to understanding galactic evolution, largely because there are multiple mechanisms which should lead to their abrupt destruction, such as gas loss and vaporization from the hot intergalactic medium, yet they manage to survive long enough to form stellar populations (Cannon et al. 2011). The Galaxy Evolution Explorer (*GALEX*) space observatory provided FUV images ready for analysis (See Gil de Paz et al. (2007)). Hα images from the *WIYN* 3.5m observatory are also analyzed for comparison (See Cannon et al. (2011)). In this paper, we present the results of that analysis, as well as a comparison to the 11 Mpc Hα, and Ultraviolet Galaxy Survey (11HUGS) sample of over 400 galaxies (Lee et al. 2011; Kennicutt et al. 2008). The data set analyzed in Lee et al. (2009) includes 300 of these galaxies within 11 Mpc that are brighter than $B = 15$ mag. Many of these galaxies are dwarfs, some massive galaxies are represented and the survey includes both spiral and irregular galaxies. The smaller data set described above is the one which will be compared to the findings from SHIELD presented in this study.

The remainder of this paper is organized as follows. In Section 2, we describe the *GALEX* and *WIYN* observations and resultant data set. In Section 3, we compare the SHIELD SFRs to the 11HUGS data set and evaluate the corrections to the Hα SFR proposed in (Lee et al. 2009). We find that this conversion in fact over-corrects for Hα in the SHIELD sample, as an Hα detriment is measurable, agreeing with previous findings.

2. Methods and Results

To investigate SFRs in the SHIELD sample, we gather data from the *GALEX* far-ultraviolet (FUV, $\backsim$1500 Å) band as well as the *WIYN* Hα data. The UV and Hα SFRs were measured separately, then compared. The near-ultraviolet (NUV, $\backsim$2200 Å) is not relevant for the purposes of this paper, since SFR is only measured from the FUV, but values are included in Table 1 for completeness since they are a fundamental portion of the *GALEX* data set for each galaxy. All of the SHIELD galaxies are available in this archive except for AGC 749237, which has not been observed yet. No FUV SFRs were obtained for this galaxy. The procedure closely follows Lee et al. (2009). Images from the survey with the longest integration time were chosen for each galaxy; the integration times are listed in Table A. Using the longest available integration times ensures a more comprehensive view of the galaxy since more flux is captured in the image. The calibration and data products of the *GALEX* GR6 data pipeline are explained in detail in Morrissey et al. (2007). Hα($\backsim$ 6576 Å) and R-band ($\backsim$6393 Å) data was gathered using the *WIYN* 3.5m ground-based telescope in 2010 and 2011. AGC 749241 could not be observed and does not appear among the Hα measurements.

First, we measure the flux in each galaxy from the *GALEX* FUV images. This is accomplished through an IDL (Interactive Data Language) code which eliminates foreground sources above a 2σ detection outside of a user-drawn object around the galaxy. Then, user-specified elliptical apertures measure both the flux within the galaxy and the background flux, subtracting the background from the galactic flux. Each flux is corrected for internal extinction based on maps from Schlegel et al. (1998)), with E(B-V) values listed in Table 1. The extinction correction is as follows:

$$m_{UV} = m_{0UV} - 7.9 \times E(B - V) \tag{1}$$

m_{0UV} is the zero point magnitude. $m_{0FUV} = 18.82$ and $m_{0NUV} = 20.08$ for *GALEX* data (Morrissey et al. 2007). Extinction-corrected fluxes are converted to luminosities using the distances in Table 1 taken from tip of the red giant branch (TRGB) analysis. The corrected Hα images from *WIYN* were analyzed with a similar technique to the FUV images. In accordance with Lee et al. (2009), the Hα values were not extinction-corrected; this is necessary to provide an averaged long-term SFR, and follows the assumptions from Kennicutt (1998), namely the difficulties in modeling extinction from integrated spectra addressed in that paper. The measured Hα fluxes were converted to luminosities, then SFRs, by a process similar to the FUV data, only with a different luminosity to SFR conversion factor.

Both conversion factors are based upon a fit from interstellar mass function (IMF) models originally discussed in Kennicutt et al. (1994):

$$SFR(M_{\odot}yr^{-1}) = 1.4 \times 10^{-28} L_{\nu}(UV)(ergs^{-1}Hz^{-1}) \tag{2}$$

$$SFR(M_{\odot}yr^{-1}) = 7.9 \times 10^{-42} L_{H\alpha}(ergs^{-1}) \tag{3}$$

These SFR conversions give the star formation rate in solar masses per year. Each assumes a constant star formation history (SFH) over ∼100 Myr in a normal disk, using a Salpeter IMF over $m = 0.1$-$100 M_{\odot}$, as discussed in Kennicutt (1998), and assuming solar metallicity. Results for each SFR measurement are presented in Table 2 and Figure 2.

Lee et al. (2009), also using the Kennicutt (1998) equations, observes a systematic decline in Hα in galaxies with low SFRs (log (SFR)∽ -1.5), and develops a corrected Hα SFR conversion, to be used for a non-dust corrected luminosity $L(H\alpha) \leq 2.5{\times}10^{39}$ erg s^{-1}:

$$log(SFR(M_{\odot}yr^{-1})) = 0.62log(7.9 \times 10^{-42} \times L(H\alpha)(ergs^{-1})) - 0.47 \tag{4}$$

This equation is based on a linear least squares fit of log[L(Hα)] versus log[SFR (M$_{\odot}$ yr^{-1})] from the 11HUGS sample Lee et al. (2009). It has also been applied to the entire SHIELD sample, listed in Table 2 and plotted on Figure 3. This metric causes the SHIELD data points to shift closer to the least squares bisector. Since the largest $L(H\alpha) = 5.21{\times}10^{38}$ erg s^{-1}, this result is predicted in Lee et al. (2009).

3. Discussion: Comparison to the 11HUGS Data Set

Computing the FUV and Hα SFRs for the twelve SHIELD galaxies, we find that the correction for declining Hα-to-FUV ratio among low-mass galaxies brings the SHIELD data set closer to the fit described by Lee et al. (2009), as illustrated in Figure 3. The standard

Kennicutt (1998) conversion is not sufficient to describe these galaxies, in agreement with results from Lee et al. (2009) regarding the Hα detriment. Considering the generally low luminosities in the SHIELD sample, which should be congruent with the results in Lee et al. (2009), this result supports previous work. Figure 2 shows that the ten SHIELD galaxies for which FUV and Hα data is available are all situated above the least squares bisector from the 11HUGS sample. Applying the corrected Hα metric suggested in Lee et al. (2009), shown in Figure 3, shifts the data points closer to the least squares bisector and corrects for the observed Hα detriment.

The SHIELD sample is not extraordinarily UV-bright, though it may still display a "bursty" SFH (Lee et al. 2009). In particular, the recent formation of a massive star would result in a significantly large $LH\alpha$, since Kennicutt (1998) assumes a constant SFH. This may explain why AGC 731457 (the most luminous galaxy) still lies far above the rest of the data set after applying the Lee correction. Lee et al. (2009) also calculates an updated SFR metric with the assumption that long-term star formation is averaged. One large star formation event in a low-mass dwarf produces enough ionized gas to significantly increase L(Hα). In this instance, the Hα correction from Lee et al. (2009) generates an Hα SFR in closer agreement with the FUV SFR. Yet, the Lee et al. (2009) metric may need further refinement in defining a low-luminosity limit for the detriment; a higher-order polynomial may be necessary to accurately correct for very luminous dwarfs.

It appears that the conversion recipe offered in Lee et al. (2009) is a reliable SFR metric for low-luminosity galaxies. However, it may be necessary to refine the conversion given in Equation 4 further, including higher order terms. Lee et al. (2009) hints at the possibility of a calibration using a polynomial in the fifth order, but does not implement this fit. This revision would likely redefine a luminosity threshold where such a conversion is applicable.

4. Summary and Conclusions

We present the FUV and Hα SFR values for the SHIELD galaxies Cannon et al. (2011), based on images from the *GALEX* survey as well as the *WIYN* 3.5m telescope. The primary result from this analysis is that the SHIELD galaxies show the Hα detriment that Lee et al. (2009) predicts. Therefore, Lee et al. (2009) SFR conversion recipes are an adequate Hα SFR predictor for these galaxies, although some revision may still be appropriate according to that study.

Further analysis of the structure of the SHIELD galaxies is needed to understand the nature of starburst star formation in this sample, and a larger sample of extremely low-mass dwarfs would offer a better understanding of general SFR trends. Kennicutt (1998) incorporates FIR luminosities to derive starburst SFRs, and to develop a more accurate SFR metric in the case of exceptionally UV-bright galaxies. Examining the spatial distribution of UV-bright and Hα-bright regions, as suggested in Lee et al. (2009) may also provide clues on the nature of star formation in these low-mass dwarfs. Cannon et al. (2011) also encourages and further describes the implications of this in-depth analysis. Such an investigation may demystify the continued survival of dwarf galaxies, offering greater insights to the cumulative understanding of galactic evolution.

5. Acknowledgments

I would like to thank Dr. John Cannon for acting as my research mentor, the SHIELD team past and present, as well as Macalester College and NSF for providing the funding for this REU. I would also like to thank the anonymous referees for providing insightful comments and criticism.

REFERENCES

Cannon, J.M., et al., 2011, ApJ, **739**, L22

Gil de Paz, A., et al., 2007, ApJS, **173**, 185

Giovanelli, A., et al., 2005, AJ, **130**, 2598

Kennicutt, R.C., 1998, ApJ, **498**, 541

Kennicutt, R.C., et al., 2008, ApJS, **178**, 247

Kennicutt, R.C., Tamblyn, P., Congdon, C.W., 1994, ApJ, **435**, 22

Lee, J.C., et al., 2009, ApJ, **706**, 599

Lee, J.C., et al., 2011, ApJS, **192**, 6

Morrissey, P., et al., 2007, ApJS, **173**, 682

Schlegel, D.J., Finkbeiner, D.P., Davis, M., 1998, ApJ, **500**, 525

This preprint was prepared with the AAS LaTeX macros v5.2.

Table 1. SHIELD UV Data

AGC	Image Integration Time (s)	α (J2000)[a]	δ (J2000)[a]	D(Mpc)[b]	E(B-V)[c]	m_{FUV}	m_{NUV}
110482	1601.1	01:42:17.4	26:22:00	8.0±0.1	0.092	18.23±0.03	17.94±0.03
111164	2268.1	02:00:10.1	28:49:52	4.9±0.1	0.055	19.24±0.05	18.78±0.03
111946	1531.6	01:46:42.2	26:48:05	8.4±0.1	0.082	19.14±0.04	19.07±0.04
111977	1702.1	01:55:20.2	27:57:14	5.4±0.1	0.070	18.22±0.05	17.78±0.03
112521	1233.3	01:41:07.6	27:19:24	5.9±0.1	0.064	20.68±0.15	20.04±0.04
174585	2531.4	07:36:10.3	09:59:11	7.7±0.1	0.038	19.23±0.02	18.69±0.06
174605	126.0	07:50:21.7	07:47:40	9.6±0.1	0.023	19.23±0.02	19.21±0.04
182595	1689.0	08:51:12.1	27:52:48	8.6±0.1	0.042	19.04±0.03	18.64±0.07
731457	1655.1	10:31:55.8	28:01:33	10.5±0.1	0.028	17.86±0.05	17.62±0.13
748778	1677.1	00:06:34.3	15:30:39	6.4±0.1	0.064	19.88±0.03	19.78±0.04
749237	...	12:26:23.4	27:44:44	18.1±0.6	0.019	...	...
749241	2785.1	12:40:01.7	26:19:19	4.3[d]	0.015	19.58±0.03	19.35±0.05

[a]See Cannon et al. (2011).

[b]These values are MATCH distances derived from Hubble observations.

[c]Extinction values based on Schlegel et al. (1998)

[d]AGC 749241 was not observed in the HST run and this value is derived from flow model estimates.

Note. — The positions, distances, *GALEX* FUV integration times, extinction values, and FUV and NUV apparent magnitudes for the twelve SHIELD galaxies. AGC 749237 was not available in the *GALEX* archive.

Table 2. FUV SFR Estimates

AGC	FUV Luminosity[e]	$\log(\mathrm{SFR})_{FUV}$
110482	1.42±0.17	-1.70±0.02
111164	2.10±0.07	-2.53±0.03
111946	6.77±0.20	-2.02±0.03
111977	6.52±0.22	-2.04±0.03
112521	0.81±0.06	-2.95±0.07
174585	5.23±0.09	-2.14±0.02
174605	8.13±0.12	-1.94±0.02
182595	7.78±0.15	-1.96±0.02
731457	34.3±1.02	-1.32±0.03
748778	1.99±0.04	-2.56±0.02
749237	...	...
749241	1.18±0.02	-2.78±0.02

[e]Units of $\times 10^{25}$ erg sec^{-1} Hz^{-1}

Note. — *GALEX* FUV luminosities, as well as the FUV SFR computed from the Kennicutt (1998) metric. AGC 749237 has not yet been observed using *GALEX* and a FUV SFR cannot be determined.

Table 3. Hα SFR Estimates

AGC	Hα Luminosity[f]	log(SFR) $H\alpha_1$[g]	log (SFR) $H\alpha_2$[h]
110482	11.6±0.31	-3.04±0.03	-2.35±0.03
111164	2.99±0.06	-3.63±0.02	-2.72±0.02
111946	3.04±0.17	-3.49±0.06	-2.71±0.06
111977	4.04±0.10	-3.49±0.03	-2.64±0.03
112521	0.63±0.08	-4.31±0.13	-3.14±0.13
174585	5.39±0.21	-3.37±0.04	-2.56±0.04
174605	4.41±0.11	-3.46±0.03	-2.61±0.03
182595	22.3±0.18	-2.75±0.01	-2.18±0.01
731457	11.7±0.13	-3.03±0.01	-2.35±0.01
748778	0.10±0.05	-5.11±0.50	-3.64±0.50
749237	52.1±0.78	-2.39±0.02	-1.95±0.02
749241	...	...	...

[f]Units of $\times\ 10^{37}$ erg sec^{-1}

[g]Computed from the Kennicutt (1998) metric.

[h]Computed from the Lee et al. (2009) prescription.

Note. — A table showing the Hα luminosities derived from *WIYN* data, as well as the Hα SFRs from both Kennicutt (1998) and Lee et al. (2009). Both of these values are plotted against the FUV SFRs in Table 2, on Fig. 2 and Fig. 3, respectively. AGC 749241 was clouded out in the *WIYN* Hα observing run and does not appear in this table.

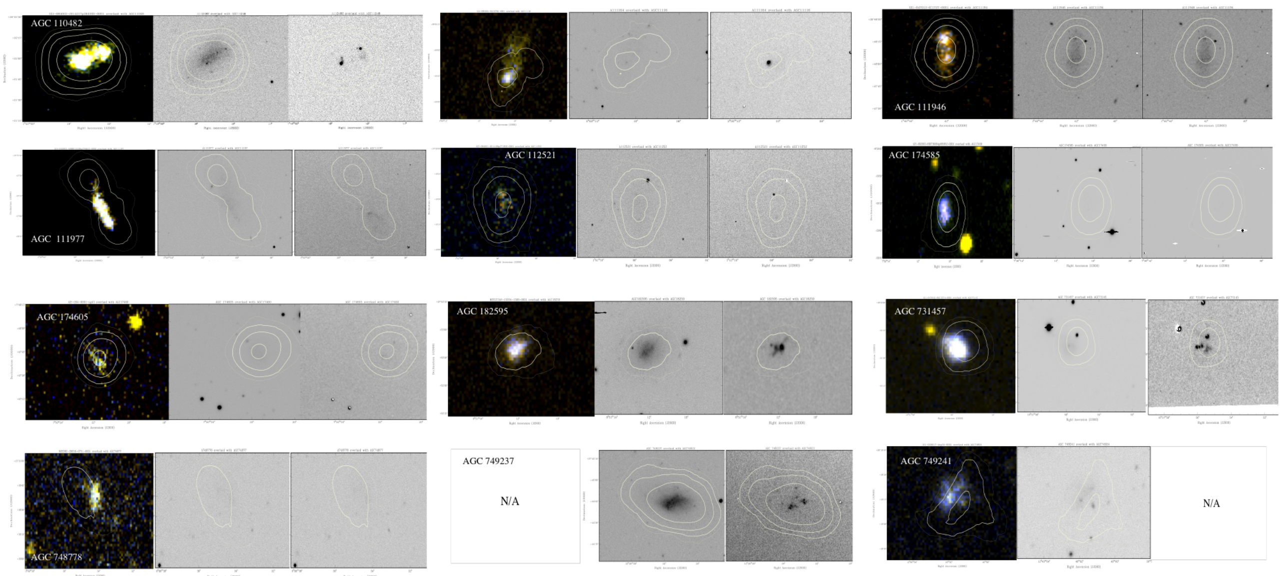

Fig. 1.— All twelve shield galaxies presented, from left to right, in the *GALEX* FUV, *WIYN* R-band, and *WIYN* Hα. AGC 749237 was not available in theGALEX archive, and AGC 749241 was clouded out in the Hα observing run. The beige contours are *JVLA* HI column density contours at (0.5, 1, 2, 4) $\times$ 10^{20} cm^{-2} levels from Cannon et al. (2011).

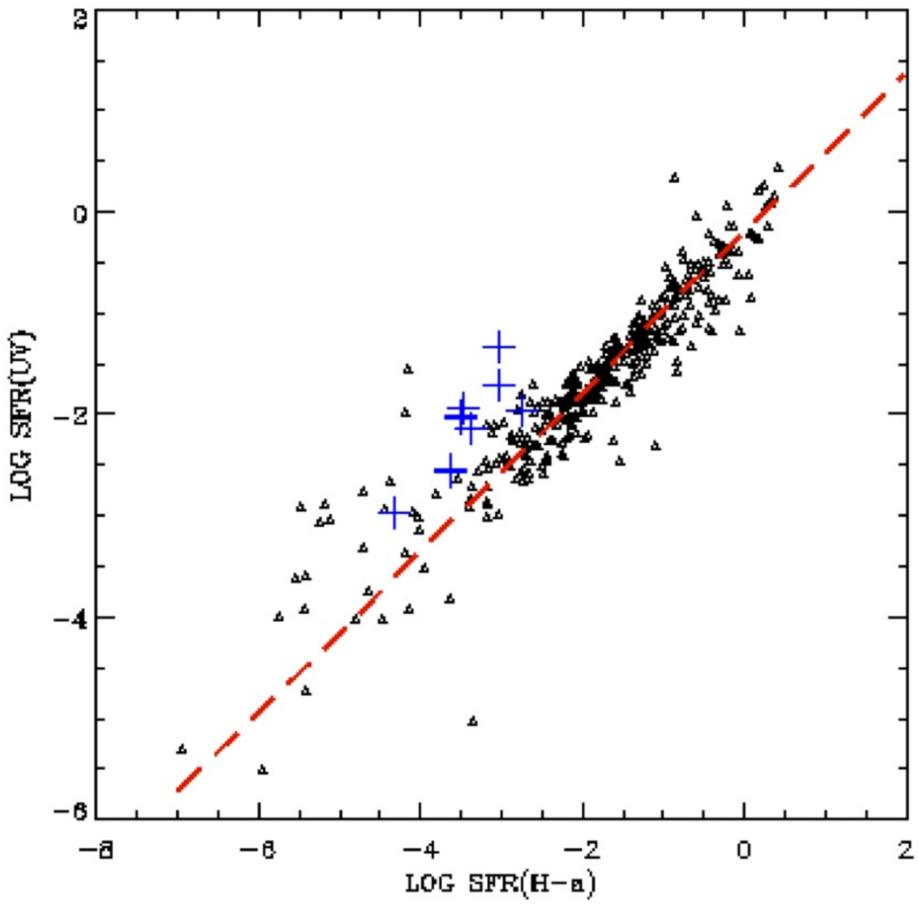

Fig. 2.— The ten SHIELD galaxies for which both Hα and FUV SFRs are available (see Table 2) are represented as blue crosses against the larger 11HUGS data set, in black, from Lee et al. (2009). Both samples are corrected for extinction but not internal dust attenuation. The least squares bisector, log(SFR)FUV - 0.79$\times$log(SFR)Hα - 0.20 is plotted in red. This line represents a best fit of the data from Lee et al. (2009). All SFRs are calculated using Kennicutt (1998) conversions.

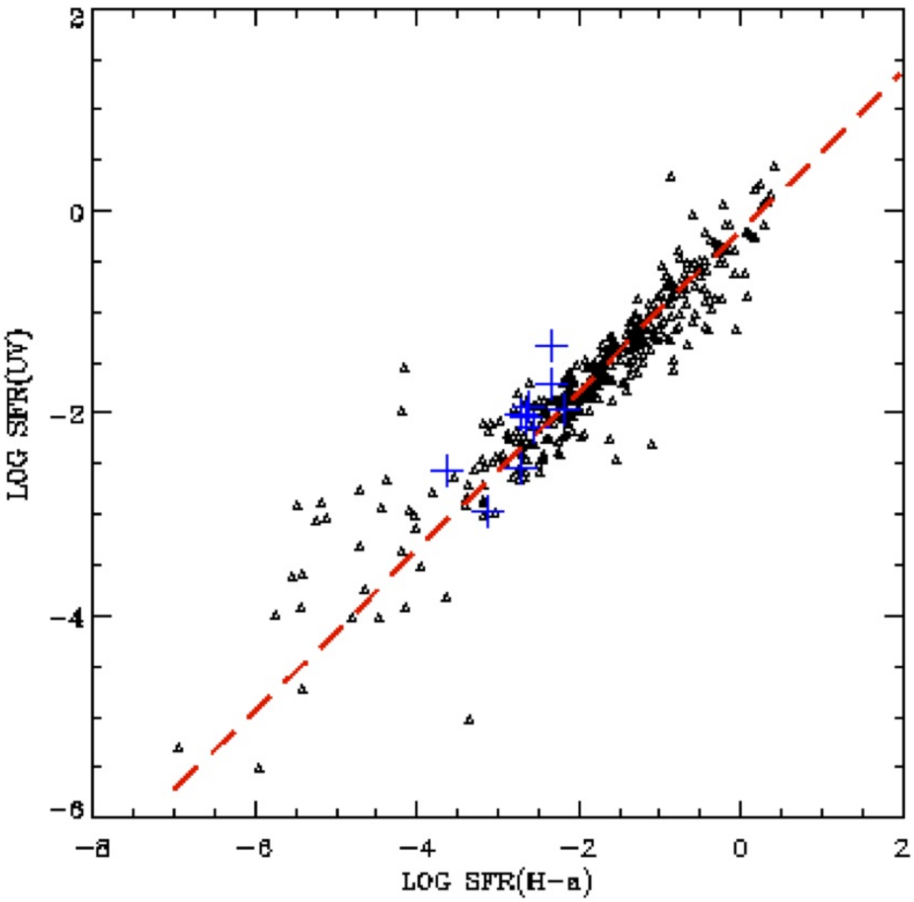

Fig. 3.— A plot with the same 11HUGS fit line and data points as Fig.1, as well as the SHIELD SFRs calculated from the updated Lee et al. (2009) metric. It appears that this metric generally corrects for the Hα SFR, as these values are in better agreement with the least squares bisector than the values in Figure 2

.